



Alkyl nitrates in the boreal forest: Formation via the NO_3 , OH and O_3 induced oxidation of BVOCs and ambient lifetimes

Jonathan Liebmann¹, Nicolas Sobanski¹, Jan Schuladen¹, Einar Karu¹, Heidi Hellén², Hannele Hakola², Qiaozhi Zha³, Mikael Ehn³, Matthieu Riva⁴, Jonathan Williams¹, Horst Fischer¹, Jos Lelieveld¹ and John N. Crowley¹

¹Division of Atmospheric Chemistry, Max Planck Institut für Chemie, 55128, Mainz, Germany

²Finnish Meteorological Institute, 00560, Helsinki, Finland

³Institute for Atmospheric and Earth System Research / Physics, University of Helsinki, 00014, Helsinki, Finland

10 ⁴University of Lyon, Université Claude Bernard Lyon1, CNRS, IRCELYON, F-69626, Villeurbanne, France
Correspondence to: John Crowley (john.crowley@mpic.de)

Abstract. The formation of alkyl nitrates in various oxidation processes taking place throughout the diel cycle can represent an important sink of reactive nitrogen and mechanism for chain-termination in atmospheric photo-oxidation cycles. The low volatility alkyl nitrates formed from biogenic volatile organic compounds (BVOCs), especially terpenoids, enhance rates of production and growth of secondary organic aerosol. Measurements of the NO_3 -reactivity and the mixing ratio of total alkyl nitrates (ΣANs) in the Finnish boreal forest enabled assessment of the relative importance of NO_3 -, O_3 - and OH-initiated formation of alkyl-nitrates from BVOCs in this environment. The high reactivity of the forest air towards NO_3 resulted in reactions of the nitrate radical with terpenes contributing substantially to formation of ANs not only during the night but also during daytime. Overall, night-time reactions of NO_3 accounted for 49% of the local production rate of ANs, with contributions of 21%, 18% and 12% for NO_3 , OH and O_3 , during the day. The lifetimes of the gas-phase ANs formed in this environment were of the order of 2 hours implying that the lifetime of NO_x is strongly controlled by biogenic emissions from the forest. As the organic nitrates are lost to the particle phase and via dry-deposition to foliar surfaces, the overall result is transfer of reactive nitrogen from anthropogenic sources to the forest ecosystem.



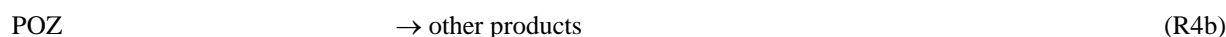
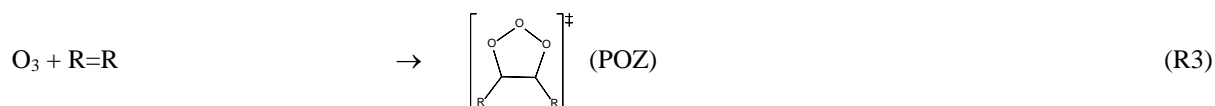
1 Introduction

Alkyl nitrates (ANs, $R\text{-CH}_2\text{ONO}_2$) are formed in chain terminating reactions that limit photochemical cycling of organic and HO_x radicals and represent an important sink for atmospheric nitrogen (Liu et al., 2012; Lee et al., 2016; Huang et al., 2019). During daytime, ANs are formed in a minor branch of the reaction of NO with organic peroxy radicals (RO_2) (Lightfoot et al., 1992), which are formed mainly via the OH-initiated oxidation of volatile organic compounds (VOCs):



The yield of ANs in reactions R1-R2 varies with the structure of the R-substituent, temperature and pressure and for small alkyl groups (e.g. $R = \text{H}, \text{CH}_3, \text{C}_2\text{H}_5$) is generally less than a few percent at 1 bar and 298 K but may increase to values close to 20% for RO_2 formed from the OH-initiation of biogenic VOCs (Perring et al., 2013; Lee et al., 2014b; IUPAC, 2019).

In the boreal forest, the reaction with O_3 represents an additional sink for biogenic VOCs (BVOCs) (Peräkylä et al., 2014; Yan et al., 2016) which, in the presence of NO can also lead to the formation alkyl nitrates. The reaction proceeds by initial addition of O_3 to the $\text{C}=\text{C}$ bond of e.g. a terpene to form a primary ozonide (POZ, R3) which rapidly decompose (R4) via Criegee intermediates to form OH and (in the presence of O_2) RO_2 . The latter react via R1 and R2 to form alkyl nitrates.



At night-time, photochemically generated OH radicals are absent and the NO_3 radical, formed by the oxidation of NO_2 by ozone (Reaction R5), is the main initiator of oxidation of several classes of VOCs with Reaction (R6a) the dominant pathway for alkyl nitrate formation (Rosen et al., 2004; Crowley et al., 2010; Rollins et al., 2013; Sobanski et al., 2017).



Reaction 6a, is a composite process involving initial formation of a nitroalkyl radical (via electrophilic addition of NO_3 to a $\text{C}=\text{C}$ double bond) followed by the formation of a nitrooxyperoxy radical (via further addition of O_2) which can react with NO, NO_3 , HO_2 or RO_2 to form substituted alkyl-nitrates (IUPAC, 2019).

The branching ratio to AN formation is generally much larger than that for organic peroxy radicals reacting with NO and for biogenic VOCs (BVOCs) can approach 80% (Ng et al., 2017; IUPAC, 2019). The formation of ANs via the degradation of saturated and unsaturated VOCs initiated by NO_3 , OH and O_3 are summarized in Fig. 1.



During daytime, the reactions of NO_3 with VOCs are often reduced in importance by the rapid photolysis of NO_3 and by its reaction with NO (R7-R9)(Wayne et al., 1991).



The fraction (f) of NO_3 radicals that undergo reaction with VOCs can be calculated according to Eq. 1

$$f = \frac{k_{\text{OTG}}^{\text{NO}_3}}{k_{\text{OTG}}^{\text{NO}_3} + J_{\text{NO}_3} + k_7[\text{NO}]} \quad (1)$$

where $k_{\text{OTG}}^{\text{NO}_3}$ is the first-order loss-frequency for NO_3 reaction with organic trace gases (NO_3 -reactivity), J_{NO_3} is the photolysis rate constant and $[\text{NO}]k_7$ the NO concentration multiplied by the rate constant for Reaction (R7). Recent measurements of NO_3 -reactivity in forested regions (Liebmann et al., 2018a; Liebmann et al., 2018b) suggest that, even during the day, a significant fraction of the nitrate radicals generated in Reaction (R5) can react with BVOCs rather than undergoing photolysis or reaction with NO to re-form NO_x ($\text{NO}_x = \text{NO} + \text{NO}_2$). During a 2016 field intensive in the boreal forest (IBAIRN, Influence of Biosphere-Atmosphere Interactions on the Reactive Nitrogen budget), we showed that, on average more than 20% of NO_3 radicals formed during the day were lost due to reaction with BVOCs (Liebmann et al., 2018a). In this work, we examine the contribution of the NO_3 -initiated oxidation of VOCs to the formation of ANs both during the day- and night-time during IBAIRN and compare this to AN formation initiated by reactions of OH and O_3 . Using calculations of the overall production rate of ANs (from OH and NO_3) and measurements of the summed mixing ratio of ANs (ΣANs), we derive a lifetime for ANs in this environment.

2 Measurements

- 20 The measurements were made during the IBAIRN field intensive in September 2016 at the “Station for Measuring Forest Ecosystem-Atmosphere Relations II” (SMEAR II) in Hyytiälä (61°51'N, 24°17'E) in southern Finland. A detailed description of the measurement site can be found elsewhere (Rinne et al., 2005; Lappalainen et al., 2009; Aaltonen et al., 2011). Briefly, the measurement site is located in the boreal forest with mostly biogenic influences. Anthropogenic emissions from two larger cities (Tampere and Jyväskylä) and a local sawmill occasionally impacted the site.
- 25 The IBAIRN campaign took place in the transition between summer and autumn with the length of day shortening from 14.0 h at the beginning of the campaign to 11.5 h at the end. Campaign temperatures, relative humidity, wind-speed and direction can be found in Fig. S1 of the supplementary information. During IBAIRN, the diel temperature varied from a night-time minimum of 2°C to a daytime maximum of 20°C, with the nights often characterized by a strong temperature inversion and a very shallow boundary layer, which resulted in higher monoterpene mixing ratios than during daytime. The relative humidity
- 30 reached 100% in many nights with ground-level fog formation. There was no rainfall during the campaign and the wind was predominantly from north-western directions with wind-speeds never exceeding 5 m s⁻¹. The NO_x levels during the entire



campaign were low (300 pptv) only increasing when the site experienced air masses with trajectories that passed over industrial regions. Daily O₃ maxima were 30-35 ppbv, with much lower values (5-10 ppbv) on those nights with strong temperature inversions (Liebmann et al., 2018a).

The mixing ratios of OH, NO, NO₂, O₃, ΣANs, VOCs, the NO₃ photolysis frequency and the NO₃-reactivity are required to examine the formation and loss of ANs during IBAIRN. Most instruments used for the data analysis sampled from a common inlet (at 8 m height) on a clearing within the boreal forest. Exceptions were measurement of some organic trace gases and the measurements of actinic flux (see below). As the instruments have been described previously (Liebmann et al., 2018a), we list only the limits of detection (LOD) and 2σ total uncertainty here.

NO was measured using a modified commercial chemi-luminescence detector (LOD = 5 pptv in 60 s, 2σ = 20%). O₃ was measured by optical absorption (LOD = 1 ppbv in 10 s, 2σ = 5%). NO₂ (LOD = 60 pptv in 6 s, 2σ = 6%) and ΣANs (LOD = 40 pptv in 10 min, 2σ = 20%) were measured using the 5-channel, thermal dissociation-cavity ring down spectrometer (TD-CRDS) described in detail by Sobanski et al. (2016). The TD-CRDS instrument also indicated that NO₃ levels were < 1 pptv throughout the campaign.

J_{NO_3} was calculated from actinic flux measured at 35 m height using a spectral radiometer (Metcon GmbH) and evaluated NO₃ cross sections / quantum yields (Burkholder et al., 2015). Ultraviolet-B radiation (280-320 nm) was sampled at 18 m height (Solar Light SL501A radiometer). NO₃-reactivity was measured with a recently developed instrument coupling a flow-tube reactor with CRDS (Liebmann et al., 2017; Liebmann et al., 2018a; Liebmann et al., 2018b). Isoprene and monoterpenes were measured from a common inlet using a Gas-Chromatograph/Atomic emission detector (GC-AED, LOD 1 pptv in 20 min, 2σ 14%), as described in (Liebmann et al., 2018a). Organic acids, alcohols, aldehydes as well as several alkanes were measured on the same clearing but at 1.5 m height, roughly 30 m away from the common inlet using a Gas-Chromatograph / Mass Spectrometer set up (GC-MS). Details are found Hellén et al. (2018)). OH radical concentrations were not directly measured during IBAIRN but obtained from a correlation of ground-level OH-measurements with ultraviolet B radiation intensity ([UVB], in units of W m⁻²) at this location with [OH] = 5.62 × 10⁵ [UVB]^{0.62} (Rohrer and Berresheim, 2006; Petäjä et al., 2009; Hellén et al., 2018). The calculated, ground level OH concentrations were multiplied by a factor 2 to take gradients in OH between ground-level and at canopy height into account (Hens et al., 2014). The OH concentrations are associated with an uncertainty of ≈ 50%.

Real-time measurements of gas- and particle phase oxidation products formed in the boreal forest were conducted using an Aerodyne high-resolution long time-of-flight chemical ionization mass spectrometer (HR-L-ToF-CIMS), equipped with iodide (I⁻) reagent ion chemistry (Lopez-Hilfiker et al., 2014; Lopez-Hilfiker et al., 2015; Lee et al., 2016; Riva et al., 2019). The instrument was coupled to a Filter Inlet for Gases and AEROSols (FIGAERO). Analyses were restricted to ions containing an iodide adduct, which guarantees detection of the parent organic compounds without substantial fragmentation. Iodide-CIMS has been described previously and demonstrated high sensitivity towards oxygenated organic compounds including alkyl nitrates both in the gas and particle phases.



3 Results and discussion

3.1 ANs production from NO₃ reactions with VOCs

In Fig. 2 we display a time series of the NO₃ precursors (NO₂ and O₃) and the NO₃-reactivity ($k_{\text{OTG}}^{\text{NO}_3}$) together with the NO₃ loss rate constant resulting from its reaction with NO and photolysis. The latter also serves to delineate day ($J_{\text{NO}_3} \geq 5 \times 10^{-4}$ s⁻¹) and night.

The instantaneous production rate of ANs from the reaction of NO₃ with VOCs ($\sum P_{\text{ANs}}^{\text{NO}_3}$) is given by:

$$\sum P_{\text{ANs}}^{\text{NO}_3} = \bar{\alpha}^{\text{NO}_3} f[\text{O}_3][\text{NO}_2]k_5 \quad (2)$$

where α^{NO_3} is a VOC dependent AN-yield. Assuming that all the VOCs responsible for loss of NO₃ were identified and quantified we can define an average yield ($\bar{\alpha}^{\text{NO}_3}$, Eq. 3) from VOC- specific values of $\alpha_i^{\text{NO}_3}$ weighted by their relative contribution to $k_{\text{OTG}}^{\text{NO}_3}$.

$$\bar{\alpha}^{\text{NO}_3} = \frac{\sum \alpha_i^{\text{NO}_3} k_i^{\text{NO}_3} [\text{C}_i]}{k_{\text{OTG}}^{\text{NO}_3}} \quad (3)$$

The rate constants and branching ratios used to calculate $\sum P_{\text{ANs}}^{\text{NO}_3}$ for individual BVOCs can be found in Table S1 of the supplementary information. A large selection of VOCs was measured but only the handful of biogenic VOCs listed contributed significantly to NO₃ reactivity.

Combining expressions (1-3), we derive:

$$\sum P_{\text{ANs}}^{\text{NO}_3} = \frac{\sum \alpha_i^{\text{NO}_3} k_i^{\text{NO}_3} [\text{C}_i]}{k_{\text{OTG}}^{\text{NO}_3} + J_{\text{NO}_3} + k_7[\text{NO}]} [\text{O}_3][\text{NO}_2]k_3 \quad (4)$$

Recognizing that $[\text{O}_3][\text{NO}_2]k_5$ and the term $(k_{\text{OTG}}^{\text{NO}_3} + J_{\text{NO}_3} + k_7[\text{NO}])$ are the total NO₃ production rates and loss rates, respectively, and that their ratio is the concentration of NO₃ in steady state, $[\text{NO}_3]_{\text{ss}}$, we can also write:

$$\sum P_{\text{ANs}}^{\text{NO}_3} = [\text{NO}_3]_{\text{ss}} \sum \alpha_i^{\text{NO}_3} k_i^{\text{NO}_3} [\text{C}_i] \quad (5)$$

Expression (5) can be used to calculate the production rates of ANs if NO₃ measurements are above the detection limit, which despite deployment of sensitive instrumentation, was not the case in IBAIRN or in previous campaigns in the boreal forest (Rinne et al., 2012; Crowley et al., 2018). This highlights the advantage of measuring the overall reactivity of NO₃ instead of its concentration in highly reactive environments.

As described by Liebmann et al. (2018a) the VOC measurements did not account for the total, measured reactivity. The reactivity that could not be attributed ($k_{\text{unattributed}}$, see eq. 6) (on average 30% at night-time and 60% during daytime) was therefore treated as stemming from a VOC with an alkyl nitrate yield of 0.7.

$$k_{\text{unattributed}} = k_{\text{OTG}}^{\text{NO}_3} - \sum k_i^{\text{NO}_3} [\text{C}_i] \quad (6)$$

A value of 0.7 was chosen as the unattributed reactivity is likely to be due to highly reactive BVOCs (e.g. terpenes that were not measured or sesquiterpenes, see Liebmann et al. (2018a)), which have alkyl nitrate yields between 0.6-0.8 (IUPAC, 2019).



The uncertainty related to the calculation of $\sum P_{\text{ANs}}^{\text{NO}_3}$ is estimated as 65% with contributions of 50% from $(k_{\text{OTG}}^{\text{NO}_3} + J_{\text{NO}_3} + k_7[\text{NO}])$, 18% from $[\text{O}_3][\text{NO}_2]k_5$, 30% from $\alpha_i^{\text{NO}_3}$, 15% from $k_i^{\text{NO}_3}$ and 15% from $[\text{C}_i]$.

3.2 ANs production from OH reactions with VOCs

The rate of production of ANs from the OH radical initiated oxidation of VOCs ($P_{\text{ANs}}^{\text{OH}}$) in the presence of NO can be calculated using Eq. 7:

$$\sum P_{\text{ANs}}^{\text{OH}} = [\text{OH}] \sum \alpha_i^{\text{RO}_2} k_i^{\text{OH}} [\text{C}_i] \quad (7)$$

where $[\text{OH}]$ is the OH concentration, $\alpha_i^{\text{RO}_2}$ the VOC-specific branching ratio for alkyl nitrate formation from the peroxy radical (RO_2) formed and $k_{\text{OTG}}^{\text{OH}}$ is the OH-reactivity derived from the VOC concentrations $[\text{C}_i]$ and the corresponding rate constant k_i^{OH} for reaction with OH.

- Organic peroxy radicals formed in reaction R1 or R4a do not react solely with NO but can also react with hydroperoxyl radicals (R10) and undergo radical recombination (R11) each of which reduces the production rate of ANs via Reaction (R2a). They can also isomerize (R12) to form a more oxidized form of RO_2 .



- Although the rate constant for some cross- and self-reactions of terpene derived RO_2 are large (Berndt et al., 2018), the organic peroxide products of these reactions have only been observed in very low mixing ratios at this site (Yan et al., 2016) and, following Browne et al. (2013), we neglect the impact of Reaction (R11). We also assume that the peroxy radical formed in R12 forms an organic nitrate with the same efficiency as the parent RO_2 , so that R12 can also be neglected. To assess the influence of reaction R10 , we used the noon-time ratio of OH to HO_2 radicals derived by Crowley et al. (2018) during a campaign at the same location ($\text{HO}_2 \approx 250 \times \text{OH}$) to calculate the HO_2 concentration during IBairn from that of OH (itself calculated from actinic flux, see above). The fraction, β , of the RO_2 radicals that react with NO is then:

$$\beta = \frac{k_{\text{RO}_2+\text{NO}}[\text{NO}]}{k_{\text{RO}_2+\text{NO}}[\text{NO}] + k_{\text{RO}_2+\text{HO}_2}[\text{HO}_2]} \quad (8)$$

- β was derived by assuming a generic rate coefficient (based on rate coefficients of known RO_2 (IUPAC, 2019)) of $k_{\text{RO}_2+\text{NO}} = 8 \times 10^{-12} \text{ cm}^3 \text{ molecule}^{-1} \text{ s}^{-1}$ and $k_{\text{RO}_2+\text{HO}_2} = 1 \times 10^{-11} \text{ cm}^3 \text{ molecule}^{-1} \text{ s}^{-1}$. Campaign average values of β varied from ≈ 0.9 in the early morning (04:00 - 08:30 UTC) during the breakup of the night-time boundary layer decreasing slightly to ≈ 0.8 later in the day (09:30-16:30 UTC). Equation (7) can thus be modified to:

$$\sum P_{\text{ANs}}^{\text{OH}} = [\text{OH}] \beta \sum \alpha_i^{\text{RO}_2} k_i^{\text{OH}} [\text{C}_i] \quad (9)$$

The rate constants and branching ratios used for these calculations can be found in Table S1 of the supplementary information.

- The total OH-reactivity ($k_{\text{OTG}}^{\text{OH}}$) was calculated using the measured concentrations of monoterpenes and isoprene as other VOCs



(e.g. aldehydes, acids, alkanes, alkenes) did not contribute significantly (Fig S2). The calculated OH-reactivity from monoterpenes varied between approximately 0.2 and 2 s⁻¹ with a campaign average of ≈ 0.3 s⁻¹, in accordance with previous measurements (Hellén et al., 2018). The high value of 7 s⁻¹ on 09.09 was associated with air masses from the local sawmill. The calculated production rate of ANs formed in the OH-initiated reactions with VOCs assumes that all ambient VOCs that result in AN formation were measured.

Previous summertime comparisons of total OH-reactivity derived from VOC measurements suggests that a significant fraction of VOC reacting with OH were not identified (Nölscher et al., 2012) and that this fraction depended on the degree of heat and drought induced stress, with 58% of the measured OH-reactivity remaining unassigned to individual VOCs during “non-stressed” conditions. As OH-reactivity data is not available during IBAIRN we cannot assess which fraction of OH-reactivity could potentially be missing for the much cooler autumn conditions, but expect this to be less than the 58% reported for the warmer summer months. We show below that unattributed OH-reactivity at the 50% level, does not significantly modify our conclusions. We estimate an uncertainty in the measured OH reactivity of ≈ 70% with contributions of 50% from [OH], 30% from β, 15% from k_i^{OH} , 30% from $\alpha_i^{RO_2}$ and 25% from [C_i].

3.3 ANs production from O₃ reactions with VOCs

The production rate of alkyl nitrates generated via the reaction of O₃ with VOCs ($\sum P_{ANS}^{NO_3}$) in the presence of NO is described by Equation 10.

$$\sum P_{ANS}^{O_3} = [O_3] \beta \sum \alpha_i^{O_3} k_i^{O_3} [C_i] \alpha_i^{RO_2} \quad (10)$$

where [O₃] is the O₃ concentration, $\alpha_i^{O_3}$ is the VOC specific yield of the RO₂ radical formed in R4, $\alpha_i^{RO_2}$ the VOC specific yield of ANs from RO₂ + NO and is assumed to be the same as for OH-initiated degradation of BVOCs, $k_{OTG}^{O_3}$ is the O₃-reactivity derived from the VOC concentrations [C_i] along with the corresponding rate constant $k_i^{O_3}$ for reaction with O₃. As for OH-reactions, β is the fraction of RO₂ radicals that react with NO rather than with HO₂ or with themselves (see above). The OH radicals that are formed in reaction 4a will react according to reactions 1-2 and would also increase the alkyl nitrate yield. However, the calculated OH concentration, based on an empirical correlation of observed [OH] with the ultraviolet B radiation contains all OH sources, including reaction R4a. In order to avoid double-counting this source of OH, the RO₂ formed in the sequence R4, R1, R2 are not taken into account in Equation (10). The rate constants and branching ratios used for these calculations can be found in Table S1 of the supplementary information.

We cannot assess which fraction of O₃-reactivity could potentially be missing, hence the obtained production rates have to be considered a lower limit. The calculated O₃-reactivity is depicted in Fig. S2 of the supporting information. While OH molecules are only abundant in higher concentrations during day, O₃ is an important oxidizing agent present during day and night. At night, away from direct sources, the NO mixing ratio reduce to ≈ zero within a few minutes after sunset due to reaction with O₃ to form NO₂ and therefore the alkyl nitrate production via this channel becomes insignificant. We used the NO₃ photolysis



rate to delineate day and night and assumed that in the absence of light ($J_{\text{NO}_3} < 5 \times 10^{-4} \text{ s}^{-1}$) the NO mixing ratios are not sufficient to support production of alkyl nitrates. The uncertainty in the term $\sum P_{\text{ANS}}^{\text{O}_3}$ was determined to $\approx 60\%$ with contributions of 5% from $[\text{O}_3]$, 30% from β , 30% from $\alpha_i^{\text{O}_3}$, 15% from $k_i^{\text{O}_3}$, 30% from $\alpha_i^{\text{RO}_2}$ and 15% from $[\text{Ci}]$.

3.4 Relative importance of OH, O₃ and NO₃ initiated VOC oxidation reactions for AN formation

5 The NO₃ production rate, the OH mixing ratios and the calculated alkyl nitrate production rates from NO₃, OH and O₃ are depicted in Fig. 3. In this NO_x-limited environment, the NO₃ production rate is highly correlated with NO₂ mixing ratios, while the OH mixing ratio is directly coupled to solar radiation. The rate of production of ANs from ozonolysis of BVOC is lowest at noon, with maximum values observed in the late afternoon.

The largest production rates of ANs are observed at night-time via NO₃ reactions though $\sum P_{\text{ANS}}^{\text{NO}_3}$ is highly variable with values
 10 between ≈ 5 and 65 pptv h⁻¹. In contrast, daytime production via OH ($\sum P_{\text{ANS}}^{\text{OH}}$) is rather reproducible with maximum values of about 21 pptv h⁻¹ at local noon. On cloudy days (e.g. 10th and 15th Sept), the OH production rate is reduced significantly and at the same time the NO₃ photolysis rate decreases so that its reactions with VOCs become more important. Both effects combine to enhance the rate of AN generation via NO₃ over that of OH. $\sum P_{\text{ANS}}^{\text{O}_3}$ can reach up to 16 pptv h⁻¹ in the late afternoon but is usually between 3-5 pptv h⁻¹. Figure 3 also plots the time series of $\sum \text{ANs}$ during the campaign. The mixing ratios of
 15 $\sum \text{ANs}$ are generally very low, and are sometimes at (or close to) the instrument's limit of detection.

The campaign-averaged contribution of OH, O₃ and NO₃ to the production of ANs during IBAIRN is displayed as a diel-profile in Fig. 4. The night-time generation of ANs formed via NO₃ reaction with BVOCs maximises at ≈ 20 pptv h⁻¹ (at $\approx 19:00$) which can be compared to the maximum value of just 10 pptv h⁻¹ from OH-reactions and 6 pptv h⁻¹ from O₃-reactions during the day. The daytime generation of ANs from NO₃ reactions is significant and at times approaches 50% of the overall
 20 rate of AN formation.

The total contributions of OH-, O₃- and NO₃-induced alkyl-nitrate formation are summarized in pie-chart form in Fig. 5. In total, 51% of ANs were formed during the day, with 21% initiated by NO₃, and 18% initiated by OH chemistry and 12% initiated by O₃ chemistry. At night-time the ANs production rate (via NO₃-initiated reactions) contributes 49%.

25 So far we have assumed that the measured VOCs account for the entire reactivity of the OH radical. If, for example, 50% of the OH-reactivity were not accounted for by the measured VOCs (see section 3.2) the contribution of OH would increase from 18% to 31% with the contributions of NO₃ decreasing to 18% (day) and 41% (night). The contribution of O₃ would decrease to 10%. This does not change the conclusion that NO₃ reactions contribute substantially to daytime AN formation in this environment.

30 Ideally, when comparing the relative contributions of day- and night-time processes to AN formation, we also need to consider the relative volumes of air throughout which the chemistry is taking place. A very rough estimation of how variations in the boundary-layer height can impact on the results can be gained by scaling the alkyl nitrate production rates by the height of the



fully developed boundary layer during IBAIRN which were 570 m during the day, and 34 m during the night (Hellén et al., 2018)) and integrating over the duration of the day (13h) day or the night (11 h). Inclusion of a factor ≈ 17 deeper boundary layer during the day results in drastic shift in the relative roles of NO_3 versus OH and O_3 , with only 6% of the total, boundary layer alkyl nitrate production is initiated by NO_3 reactions at night-time compared to 39% during the day. By comparison, the daytime, OH initiated formation of alkyl nitrates accounts for 33%, whereas O_3 accounts for 22% of the total. These very rough estimates can only be considered illustrative of the potential effects as they are biased by the inherent assumption that there are no vertical gradients in OH or NO_3 reactivity during day or night, which is however not to be the case (Eerdekens et al., 2009; Nölscher et al., 2012; Liebmann et al., 2018a; Zha et al., 2018) and also assumes that the daytime boundary layer reaches its fully developed height immediately after dawn. The true values will depend on the details of mixing within and development of the boundary layer and will lie between the two sets of calculations.

3.5 Lifetime of ANs

As illustrated in Fig. 3, the ΣANs mixing ratios reached maximum values of only ≈ 100 pptv despite production terms of 40 pptv h^{-1} , indicating that the lifetimes of the ANs are relatively short. If this is the case, the local concentration of ANs are largely decoupled from the effects of long range transport (timescales of days) and the AN-lifetime (τ_{ANs}) can be calculated using a stationary state approach via (Eq. 11):

$$\tau_{\text{ANs}} = \frac{[\text{ANs}]}{\Sigma P_{\text{ANs}}} \quad (11)$$

where ΣP_{ANs} is the total production rate (NO_3 , OH and O_3 initiated). The campaign averaged, diel variation of the ANs mixing ratio and ΣP_{ANs} are given in Fig. 6 (upper panel). A plot of ΣANs versus ΣP_{ANs} using the 1 h averages from the diel profiles is displayed in the lower panel of Fig. 6 with daytime data represented by the red data points and night-time data by the black data points. Within the overall uncertainty, represented by the error-bars there is no significant difference between the day- and night-time data, with a linear fit through all the data indicating a lifetime of $\approx 2 \pm 0.5$ hours or a loss rate constant of $5.6 \times 10^{-4} \text{ s}^{-1}$. The intercept of $\approx 24 \pm 5$ pptv ANs can be attributed to small, possibly mono-functional alkyl nitrates that have longer lifetimes and which therefore could have been transported to the site rather than generated locally (Clemitshaw et al., 1997; Romer et al., 2016).

We now examine the potential reasons for the short lifetime of ANs at this location. ANs react inefficiently with O_3 , OH and NO_3 and low rates of photolysis mean that their lifetimes are likely to be controlled largely by dry deposition and / or heterogeneous hydrolysis on aerosol or hydrometeors (Browne et al., 2013). In a well-mixed, daytime boundary layer the deposition velocity (V_{dep}) is equal to $k_{\text{dep}}H_{\text{BL}}$, where H_{BL} is the boundary layer height, and k_{dep} is the first-order loss rate constant due to deposition. Taking a value of $V_{\text{dep}} \approx 2$ reported for ANs in the Californian Sierra Nevada Mountains (Farmer and Cohen, 2008) and an average, noon-time boundary layer height of 570 m, we derive a lifetime w.r.t. deposition of 8 hours, substantially longer than that observed.

The contribution of loss of ANs via heterogeneous uptake to sub-micron aerosol (k_{het}) can be accessed via eq. 12.



$$k_{\text{het}} = \frac{\gamma \bar{c} A}{4} \quad (12)$$

Where γ is the uptake coefficient, A the aerosol surface area density (in $\text{cm}^2 \text{cm}^{-3}$), \bar{c} the average thermal velocity (in cm s^{-1}). For an alkyl nitrate derived from monoterpene oxidation ($\text{C}_{10}\text{H}_{14}\text{NO}_7$, (Yan et al., 2016; Lee et al., 2018)) $\bar{c} \approx 15000 \text{ cm s}^{-1}$. Taking an uptake coefficient of between 10^{-3} - 10^{-4} for water soluble organics (Wu et al., 2015; Crowley et al., 2018) an aerosol surface area of 1×10^{-5} - $2 \times 10^{-4} \text{ cm}^2 \text{cm}^{-3}$ would be required to account for loss rate constants of $5.6 \times 10^{-4} \text{ s}^{-1}$. Such aerosol surface areas are at least an order of magnitude larger than provided by submicron aerosol at this site. However, the high molecular weight, biogenically derived ANs in the boreal forest have low vapour pressures and transfer via condensation to existing particles is likely to be important. In this case transfer to the particle phase may be controlled by diffusion and accommodation and the effective uptake efficiency could be > 0.1 . Once transferred to the particle phase, a short lifetime with respect to hydrolysis to HNO_3 will result in permanent (irreversible) loss of the AN from the gas-phase (Browne et al., 2013; Lee et al., 2016; Lee et al., 2018) and eventually to deposition (as inorganic nitrate) to the plant surfaces and forest floor. The deposition of nitrate thus represents the last step in a sequence of biological and photochemical processes that enables, via emission of BVOCs, the trapping by the biosphere of reactive, gas-phase NO_x of largely anthropogenic origin and thus the transfer of nitrogen back to the ecosystem. Especially in nitrogen poor environments (e.g. at high latitudes) this presents an important route for plant and forest ground fertilization (Fowler et al.; Huang et al., 2019).

Our TD-CRDS instrument measures the total concentration of ANs, without speciation and therefore does not allow us to investigate whether ANs formed via OH-, O_3 - or NO_3 -initiated degradation of BVOCs have different lifetimes. The molecular composition of a total of 45 organic nitrates (C1-C10, O3-O8, N1) was identified using the I-CIMS, which is known to be sensitive towards alkyl-nitrates (Lee et al., 2014b; Lee et al., 2016). In the following discussion we therefore consider the masses to be associated mainly with alkyl-nitrates (and not e.g. peroxy-nitrates). Neither the absolute nor the relative sensitivity (between different alkyl-nitrates) is known and the following discussion is necessarily qualitative in nature. Assuming equal sensitivity across the mass spectrum for the I-CIMS measurements in IBARN (Lee et al., 2014a; Lee et al., 2016) we find that in total only 10% of the organic nitrates were C5, whereas C6-C10 accounted for 85% of the signal. This is indicated in Fig. S3 of the supplementary information.

In Figure 7, we compare the TD-CRDS measurement of the ΣANs measurement to signal of the I-CIMS, the latter separated into C1-C5 and C6-C10 species. As the I-CIMS data are available as counts only, we have normalised the datasets in Figure 6 to the values at 12:00 UTC. The C1-C5 and C6-C10 trace gases identified by the I-CIMS display very similar diel cycles, with daytime maxima and low values at night-time, as also seen for the ΣANs data. The I-CIMS data do however indicate a much more pronounced diel cycle, which is related to the different positions of the inlets of the instruments. Whereas the TD-CRDS sampled at a height of 8.5 m above the ground, the I-CIMS inlet was located at a height of just 1.5 m. As mentioned already, high relative humidity was frequently accompanied by ground-level fog at night-time during IBARN, which would have significantly impacted the I-CIMS dataset, resulting in lower, mean night-time signals.



Figure 8 plots the daytime and night-time campaign mean signal at each organic nitrate mass throughout the campaign. C9 and C10 nitrates provided the greatest signals on average, followed by C9 and then C7 and C8. As seen from the diel average (Fig. 7), the organic-nitrate signals were significantly larger during day than at night-time, the lowest day-to-night ratios being found among the C9 and C10 species and the largest day-night ratios found for C5 and smaller. The C5 organic nitrates (and smaller) are likely to stem from isoprene chemistry, whereas C6 and larger are likely to be products of terpene oxidation (Lee et al., 2016). Our observations are broadly consistent with the study of Huang et al. (2019) in a mixed isoprene-terpene forest, who observed daytime concentration maxima for C5-species and night-time maxima for C10. A more detailed comparison with Huang et al. (2019) is however difficult owing to very different isoprene-to-terpene emission rates, which in the IBAIRN campaign strongly favoured terpenes (Liebmann et al., 2018a).

Our observations during IBAIRN, of efficient daytime production of gas-phase ANs from NO_3 chemistry and short night-time lifetimes are entirely consistent with the results from recent studies at the IBAIRN site by Lee et al. (2018) who found that organic nitrates previously designated as resulting from night-time processing of BVOCs (Yan et al., 2016) were also present during daytime. In addition, they found relatively few organics with “night-time” character in the gas-phase compared to the aerosol-phase, indicating efficient transfer of gas-phase organic nitrates to the particle-phase at night-time, likely aided by low temperatures and high relative humidity.

In summary, during the IBAIRN campaign in the boreal forest in southern Finland (5th-22nd Sept, 2016), alkyl nitrate formation was dominated by the reaction of NO_3 radicals with monoterpenes, both during the day- and night-time, with smaller contributions from both OH and O_3 initiated oxidation of BVOCs. This result highlights the important role of daytime NO_3 chemistry (with respect to organic nitrate formation) in this environment. The short, average lifetime of ≈ 2 h for the total alkyl-nitrates (ΣANs) indicates efficient uptake to existing particles and deposition.

Data availability

The data used in this study are archived at the IBAIRN repository at the KEEPER service of the Max Planck Digital Library (<https://keeper.mpdl.mpg.de>). Contingent to agreeing with the IBAIRN data-protocol, the data will be available for external users from August 2019.

Author contributions

Jonathan Liebmann was responsible for the NO_3 -reactivity measurements and interpretation during IBAIRN and, with contributions from John Crowley, Horst Fischer and Jos Lelieveld, wrote the manuscript. Nicolas Sobanski was responsible for the CRDS measurements of ANs, NO_3 and NO_2 . Jan Schuladen was responsible for the O_3 and J-value measurements. Horst Fischer was responsible for the NO measurements. Einar Karu, Jonathan Williams



Heidi Hellén and Hannele Hakola were responsible for the VOCs and BVOCs measurements. Qiaozhi Zha and Matthieu Riva were responsible for the I-CIMS measurements of ANs. The IBairn campaign was conceived and organised by John Crowley and Mikael Ehn.

Competing interests

- 5 The authors declare that they have no conflict of interest.

Acknowledgements

We are grateful to ENVRIplus for partial financial support of the IBairn campaign. We would like to thank Uwe Parchatka for the provision of NO measurements and the excellent technical support from Janne Levula and team at Hyytiälä.

10

References

- Aaltonen, H., Pumpanen, J., Pihlatie, M., Hakola, H., Hellén, H., Kulmala, L., Vesala, T., and Bäck, J.: Boreal pine forest floor biogenic volatile organic compound emissions peak in early summer and autumn, *Agri. Forest Met.*, 151, 682-691, doi:<http://dx.doi.org/10.1016/j.agrformet.2010.12.010>, 2011.
- 15 Berndt, T., Mender, B., Scholz, W., Fischer, L., Herrmann, H., Kulmala, M., and Hansel, A.: Accretion Product Formation from Ozonolysis and OH Radical Reaction of alpha-Pinene: Mechanistic Insight and the Influence of Isoprene and Ethylene, *Env. Sci. Tech.*, 52, 11069-11077, doi:10.1021/acs.est.8b02210, 2018.
- Browne, E. C., Min, K. E., Wooldridge, P. J., Apel, E., Blake, D. R., Brune, W. H., Cantrell, C. A., Cubison, M. J., Diskin, G. S., Jimenez, J. L., Weinheimer, A. J., Wennberg, P. O., Wisthaler, A., and Cohen, R. C.: Observations of total RONO₂ over the boreal forest: NO_x sinks and HNO₃ sources, *Atmos. Chem. Phys.*, 13, 4543-4562, doi:10.5194/acp-13-4543-2013, 2013.
- 20 Burkholder, J. B., Sander, S. P., Abbatt, J., Barker, J. R., Huie, R. E., Kolb, C. E., Kurylo, M. J., Orkin, V. L., Wilmouth, D. M., and Wine, P. H.: Chemical Kinetics and Photochemical Data for Use in Atmospheric Studies, Evaluation No. 18," JPL Publication 15-10, Jet Propulsion Laboratory, Pasadena, <http://jpldataeval.jpl.nasa.gov>, 2015.
- Clemetshaw, K. C., Williams, J., Rattigan, O. V., Shallcross, D. E., Law, K. S., and Anthony Cox, R.: Gas-phase ultraviolet absorption cross-sections and atmospheric lifetimes of several C₂ - C₅ alkyl nitrates, *Journal of Photochemistry and Photobiology A: Chemistry*, 102, 117-126, 1997.
- 25 Crowley, J. N., Schuster, G., Pouvesle, N., Parchatka, U., Fischer, H., Bonn, B., Bingemer, H., and Lelieveld, J.: Nocturnal nitrogen oxides at a rural mountain site in south-western Germany, *Atmos. Chem. Phys.*, 10, 2795-2812, 2010.
- Crowley, J. N., Pouvesle, N., Phillips, G. J., Axinte, R., Fischer, H., Petäjä, T., Nölscher, A., Williams, J., Hens, K., Harder, H., Martinez-Harder, M., Novelli, A., Kubistin, D., Bohn, B., and Lelieveld, J.: Insights into HO_x and RO_x chemistry in the boreal forest via measurement of peroxyacetic acid, peroxyacetic nitric anhydride (PAN) and hydrogen peroxide, *Atmos. Chem. Phys.*, 18, 13457-13479, doi:10.5194/acp-18-13457-2018, 2018.
- 30 Eerdekens, G., Yassaa, N., Sinha, V., Aalto, P. P., Aufmhoff, H., Arnold, F., Fiedler, V., Kulmala, M., and Williams, J.: VOC measurements within a boreal forest during spring 2005: on the occurrence of elevated monoterpene concentrations during night time intense particle concentration events, *Atmos. Chem. Phys.*, 9, 8331-8350, doi:10.5194/acp-9-8331-2009, 2009.
- 35 Farmer, D. K., and Cohen, R. C.: Observations of HNO₃, ΣAN, ΣPN and NO₂ fluxes: evidence for rapid HO_x chemistry within a pine forest canopy, *Atmos. Chem. Phys.*, 8, 3899-3917, doi:10.5194/acp-8-3899-2008, 2008.



- Fowler, D., Pyle, J. A., Raven, J. A., and Sutton, M. A.: The global nitrogen cycle in the twenty-first century: introduction, Philosophical transactions of the Royal Society of London. Series B, Biological sciences, 368, 20130165-20130165, doi:10.1098/rstb.2013.0165,
- 5 Hellén, H., Praplan, A. P., Tykkä, T., Ylivinkka, I., Vakkari, V., Bäck, J., Petäjä, T., Kulmala, M., and Hakola, H.: Long-term measurements of volatile organic compounds highlight the importance of sesquiterpenes for the atmospheric chemistry of a boreal forest, Atmos. Chem. Phys., 18, 13839-13863, doi:10.5194/acp-18-13839-2018, 2018.
- Hens, K., Novelli, A., Martinez, M., Auld, J., Axinte, R., Bohn, B., Fischer, H., Keronen, P., Kubistin, D., Nolscher, A. C., Oswald, R., Paasonen, P., Petaja, T., Regelin, E., Sander, R., Sinha, V., Sipila, M., Taraborrelli, D., Ernest, C. T., Williams, J., Lelieveld, J., and Harder, H.: Observation and modelling of HOx radicals in a boreal forest, Atmos. Chem. Phys., 14, 8723-8747, doi:10.5194/acp-14-8723-2014, 2014.
- 10 Huang, W., Saathoff, H., Shen, X., Ramisetty, R., Leisner, T., and Mohr, C.: Chemical Characterization of Highly Functionalized Organonitrates Contributing to Night-Time Organic Aerosol Mass Loadings and Particle Growth, Env. Sci. Tech., 53, 1165-1174, doi:10.1021/acs.est.8b05826, 2019.
- IUPAC: Task Group on Atmospheric Chemical Kinetic Data Evaluation, (Ammann, M., Cox, R.A., Crowley, J.N., Herrmann, H., Jenkin, M.E., McNeill, V.F., Mellouki, A., Rossi, M. J., Troe, J. and Wallington, T. J.) <http://iupac.pole-ether.fr/index.html>, 2019.
- 15 Lappalainen, H. K., Sevanto, S., Bäck, J., Ruuskanen, T. M., Kolari, P., Taipale, R., Rinne, J., Kulmala, M., and Hari, P.: Day-time concentrations of biogenic volatile organic compounds in a boreal forest canopy and their relation to environmental and biological factors, Atmos. Chem. Phys., 9, 5447-5459, doi:10.5194/acp-9-5447-2009, 2009.
- 20 Lee, B. H., Lopez-Hilfiker, F. D., Mohr, C., Kurten, T., Worsnop, D. R., and Thornton, J. A.: An Iodide-Adduct High-Resolution Time-of-Flight Chemical-Ionization Mass Spectrometer: Application to Atmospheric Inorganic and Organic Compounds, Env. Sci. Tech., 48, 6309-6317, doi:10.1021/es500362a, 2014a.
- Lee, B. H., Mohr, C., Lopez-Hilfiker, F. D., Lutz, A., Hallquist, M., Lee, L., Romer, P., Cohen, R. C., Iyer, S., Kurten, T., Hu, W. W., Day, D. A., Campuzano-Jost, P., Jimenez, J. L., Xu, L., Ng, N. L., Guo, H. Y., Weber, R. J., Wild, R. J., Brown, S. S., Koss, A., de Gouw, J., Olson, K., Goldstein, A. H., Seco, R., Kim, S., McAvey, K., Shepson, P. B., Starn, T., Baumann, K., Edgerton, E. S., Liu, J. M., Shilling, J. E., Miller, D. O., Brune, W., Schobesberger, S., D'Ambro, E. L., and Thornton, J. A.: Highly functionalized organic nitrates in the southeast United States: Contribution to secondary organic aerosol and reactive nitrogen budgets, Proc. Natl. Acad. Sci. U. S. A., 113, 1516-1521, doi:10.1073/pnas.1508108113, 2016.
- 25 Lee, B. H., Lopez-Hilfiker, F. D., D'Ambro, E. L., Zhou, P., Boy, M., Petäjä, T., Hao, L., Virtanen, A., and Thornton, J. A.: Semi-volatile and highly oxygenated gaseous and particulate organic compounds observed above a boreal forest canopy, Atmos. Chem. Phys., 18, 11547-11562, doi:10.5194/acp-18-11547-2018, 2018.
- 30 Lee, L., Wooldridge, P. J., Gilman, J. B., Warneke, C., de Gouw, J., and Cohen, R. C.: Low temperatures enhance organic nitrate formation: evidence from observations in the 2012 Uintah Basin Winter Ozone Study, Atmos. Chem. Phys., 14, 12441-12454, doi:10.5194/acp-14-12441-2014, 2014b.
- 35 Liebmann, J., Karu, E., Sobanski, N., Schuladen, J., Ehn, M., Schallhart, S., Quéléver, L., Hellen, H., Hakola, H., Hoffmann, T., Williams, J., Fischer, H., Lelieveld, J., and Crowley, J. N.: Direct measurement of NO₃ radical reactivity in a boreal forest, Atmos. Chem. Phys., 2018, 3799-3815, doi:10.5194/acp-18-3799-2018, 2018a.
- Liebmann, J. M., Schuster, G., Schuladen, J. B., Sobanski, N., Lelieveld, J., and Crowley, J. N.: Measurement of ambient NO₃ reactivity: Design, characterization and first deployment of a new instrument, Atmos. Meas. Tech., 2017, 1241-1258, doi:10.5194/amt-2016-381, 2017.
- 40



- Liebmann, J. M., Muller, J. B. A., Kubistin, D., Claude, A., Holla, R., Plass-Dülmer, C., Lelieveld, J., and Crowley, J. N.: Direct measurements of NO₃ reactivity in and above the boundary layer of a mountaintop site: identification of reactive trace gases and comparison with OH reactivity, *Atmos. Chem. Phys.*, 18, 12045-12059, doi:10.5194/acp-18-12045-2018, 2018b.
- Lightfoot, P. D., Cox, R. A., Crowley, J. N., Destriau, M., Hayman, G. D., Jenkin, M. E., Moortgat, G. K., and Zabel, F.: Organic peroxy radicals - kinetics, spectroscopy and tropospheric chemistry, *Atmos. Environ., Part A*, 26, 1805-1961, 1992.
- Liu, S., Shilling, J. E., Song, C., Hiranuma, N., Zaveri, R. A., and Russell, L. M.: Hydrolysis of Organonitrate Functional Groups in Aerosol Particles, *Aerosol Science and Technology*, 46, 1359-1369, doi:10.1080/02786826.2012.716175, 2012.
- Lopez-Hilfiker, F. D., Mohr, C., Ehn, M., Rubach, F., Kleist, E., Wildt, J., Mentel, T. F., Lutz, A., Hallquist, M., Worsnop, D., and Thornton, J. A.: A novel method for online analysis of gas and particle composition: description and evaluation of a Filter Inlet for Gases and AEROSols (FIGAERO), *Atmos. Meas. Tech.*, 7, 983-1001, doi:10.5194/amt-7-983-2014, 2014.
- Lopez-Hilfiker, F. D., Mohr, C., Ehn, M., Rubach, F., Kleist, E., Wildt, J., Mentel, T. F., Carrasquillo, A. J., Daumit, K. E., Hunter, J. F., Kroll, J. H., Worsnop, D. R., and Thornton, J. A.: Phase partitioning and volatility of secondary organic aerosol components formed from alpha-pinene ozonolysis and OH oxidation: the importance of accretion products and other low volatility compounds, *Atmos. Chem. Phys.*, 15, 7765-7776, doi:10.5194/acp-15-7765-2015, 2015.
- Ng, N. L., Brown, S. S., Archibald, A. T., Atlas, E., Cohen, R. C., Crowley, J. N., Day, D. A., Donahue, N. M., Fry, J. L., Fuchs, H., Griffin, R. J., Guzman, M. I., Herrmann, H., Hodzic, A., Iinuma, Y., Jimenez, J. L., Kiendler-Scharr, A., Lee, B. H., Luecken, D. J., Mao, J., McLaren, R., Mutzel, A., Osthoff, H. D., Ouyang, B., Picquet-Varrault, B., Platt, U., Pye, H. O. T., Rudich, Y., Schwantes, R. H., Shiraiwa, M., Stutz, J., Thornton, J. A., Tilgner, A., Williams, B. J., and Zaveri, R. A.: Nitrate radicals and biogenic volatile organic compounds: oxidation, mechanisms, and organic aerosol, *Atmos. Chem. Phys.*, 17, 2103-2162, doi:10.5194/acp-17-2103-2017, 2017.
- Nölscher, A. C., Williams, J., Sinha, V., Custer, T., Song, W., Johnson, A. M., Axinte, R., Bozem, H., Fischer, H., Pouvesle, N., Phillips, G., Crowley, J. N., Rantala, P., Rinne, J., Kulmala, M., Gonzales, D., Valverde-Canossa, J., Vogel, A., Hoffmann, T., Ouwersloot, H. G., Vilà-Guerau de Arellano, J., and Lelieveld, J.: Summertime total OH reactivity measurements from boreal forest during HUMPPA-COPEC 2010, *Atmos. Chem. Phys.*, 12, 8257-8270, doi:10.5194/acp-12-8257-2012, 2012.
- Peräkylä, O., Vogt, M., Tikkanen, O. P., Laurila, T., Kajos, M. K., Rantala, P. A., Patokoski, J., Aalto, J., Yli-Juuti, T., Ehn, M., Sipilä, M., Paasonen, P., Rissanen, M., Nieminen, T., Taipale, R., Keronen, P., Lappalainen, H. K., Ruuskanen, T. M., Rinne, J., Kerminen, V. M., Kulmala, M., Back, J., and Petaja, T.: Monoterpenes' oxidation capacity and rate over a boreal forest: temporal variation and connection to growth of newly formed particles, *Boreal Environ. Res.*, 19, 293-310, 2014.
- Perring, A. E., Pusede, S. E., and Cohen, R. C.: An observational perspective on the atmospheric impacts of alkyl and multifunctional nitrates on ozone and secondary organic aerosol, *Chem. Rev.*, 113, 5848-5870, doi:10.1021/cr300520x, 2013.
- Petäjä, T., Mauldin, I. R. L., Kosciuch, E., McGrath, J., Nieminen, T., Paasonen, P., Boy, M., Adamov, A., Kotiaho, T., and Kulmala, M.: Sulfuric acid and OH concentrations in a boreal forest site, *Atmos. Chem. Phys.*, 9, 7435-7448, doi:10.5194/acp-9-7435-2009, 2009.
- Rinne, J., Ruuskanen, T. M., Reissell, A., Taipale, R., Hakola, H., and Kulmala, M.: On-line PTR-MS measurements of atmospheric concentrations of volatile organic compounds in a European boreal forest ecosystem, *Boreal Environmental Research*, 10, 425-436, 2005.
- Rinne, J., Markkanen, T., Ruuskanen, T. M., Petaja, T., Keronen, P., Tang, M. J., Crowley, J. N., Rannik, U., and Vesala, T.: Effect of chemical degradation on fluxes of reactive compounds – a study with a stochastic Lagrangian transport model, *Atmos. Chem. Phys.*, 12, 4843-4854, 2012.



- Riva, M., Heikkinen, L., Bell, D. M., Peräkylä, O., Zha, Q., Schallhart, S., Rissanen, M. P., Imre, D., Petäjä, T., Thornton, J. A., Zelenyuk, A., and Ehn, M.: Chemical transformations in monoterpene-derived organic aerosol enhanced by inorganic composition, *npj Climate and Atmospheric Science*, 2, 2, doi:10.1038/s41612-018-0058-0, 2019.
- 5 Rohrer, F., and Berresheim, H.: Strong correlation between levels of tropospheric hydroxyl radicals and solar ultraviolet radiation, *Nature*, 442, 184-187, doi:10.1038/nature04924, 2006.
- Rollins, A. W., Pusede, S., Wooldridge, P., Min, K. E., Gentner, D. R., Goldstein, A. H., Liu, S., Day, D. A., Russell, L. M., Rubitschun, C. L., Surratt, J. D., and Cohen, R. C.: Gas/particle partitioning of total alkyl nitrates observed with TD-LIF in Bakersfield, *J. Geophys. Res. -Atmos.*, 118, 6651-6662, doi:10.1002/jgrd.50522, 2013.
- 10 Romer, P. S., Duffey, K. C., Wooldridge, P. J., Allen, H. M., Ayres, B. R., Brown, S. S., Brune, W. H., Crounse, J. D., de Gouw, J., Draper, D. C., Feiner, P. A., Fry, J. L., Goldstein, A. H., Koss, A., Misztal, P. K., Nguyen, T. B., Olson, K., Teng, A. P., Wennberg, P. O., Wild, R. J., Zhang, L., and Cohen, R. C.: The lifetime of nitrogen oxides in an isoprene-dominated forest, *Atmos. Chem. Phys.*, 16, 7623-7637, doi:10.5194/acp-16-7623-2016, 2016.
- 15 Rosen, R. S., Wood, E. C., Wooldridge, P. J., Thornton, J. A., Day, D. A., Kuster, W., Williams, E. J., Jobson, B. T., and Cohen, R. C.: Observations of total alkyl nitrates during Texas Air Quality Study 2000: Implications for O₃ and alkyl nitrate photochemistry, *J. Geophys. Res. -Atmos.*, 109, Art. Nr D07303, doi:doi:10.1029/2003jd004227, 2004.
- Sobanski, N., Schuladen, J., Schuster, G., Lelieveld, J., and Crowley, J. N.: A five-channel cavity ring-down spectrometer for the detection of NO₂, NO₃, N₂O₅, total peroxy nitrates and total alkyl nitrates, *Atmos. Meas. Tech.*, 9, 5103-5118, doi:10.5194/amt-9-5103-2016, 2016.
- 20 Sobanski, N., Thieser, J., Schuladen, J., Sauvage, C., Song, W., Williams, J., Lelieveld, J., and Crowley, J. N.: Day- and Night-time Formation of Organic Nitrates at a Forested Mountain-site in South West Germany, *Atmos. Chem. Phys.*, 17, 4115-4130, 2017.
- Wayne, R. P., Barnes, I., Biggs, P., Burrows, J. P., Canosa-Mas, C. E., Hjorth, J., Le Bras, G., Moortgat, G. K., Perner, D., Poulet, G., Restelli, G., and Sidebottom, H.: The nitrate radical: Physics, chemistry, and the atmosphere, *Atmos. Env. A*, 25A, 1-206, 1991.
- 25 Wu, Q. Q., Huang, L. B., Liang, H., Zhao, Y., Huang, D., and Chen, Z. M.: Heterogeneous reaction of peroxyacetic acid and hydrogen peroxide on ambient aerosol particles under dry and humid conditions: kinetics, mechanism and implications, *Atmos. Chem. Phys.*, 15, 6851-6866, 2015.
- 30 Yan, C., Nie, W., Äijälä, M., Rissanen, M. P., Canagaratna, M. R., Massoli, P., Junninen, H., Jokinen, T., Sarnela, N., Häme, S. A. K., Schobesberger, S., Canonaco, F., Yao, L., Prévôt, A. S. H., Petäjä, T., Kulmala, M., Sipilä, M., Worsnop, D. R., and Ehn, M.: Source characterization of highly oxidized multifunctional compounds in a boreal forest environment using positive matrix factorization, *Atmos. Chem. Phys.*, 16, 12715-12731, doi:10.5194/acp-16-12715-2016, 2016.
- 35 Zha, Q., Yan, C., Junninen, H., Riva, M., Sarnela, N., Aalto, J., Quéléver, L., Schallhart, S., Dada, L., Heikkinen, L., Peräkylä, O., Zou, J., Rose, C., Wang, Y., Mammarella, I., Katul, G., Vesala, T., Worsnop, D. R., Kulmala, M., Petäjä, T., Bianchi, F., and Ehn, M.: Vertical characterization of highly oxygenated molecules (HOMs) below and above a boreal forest canopy, *Atmos. Chem. Phys.*, 18, 17437-17450, doi:10.5194/acp-18-17437-2018, 2018.

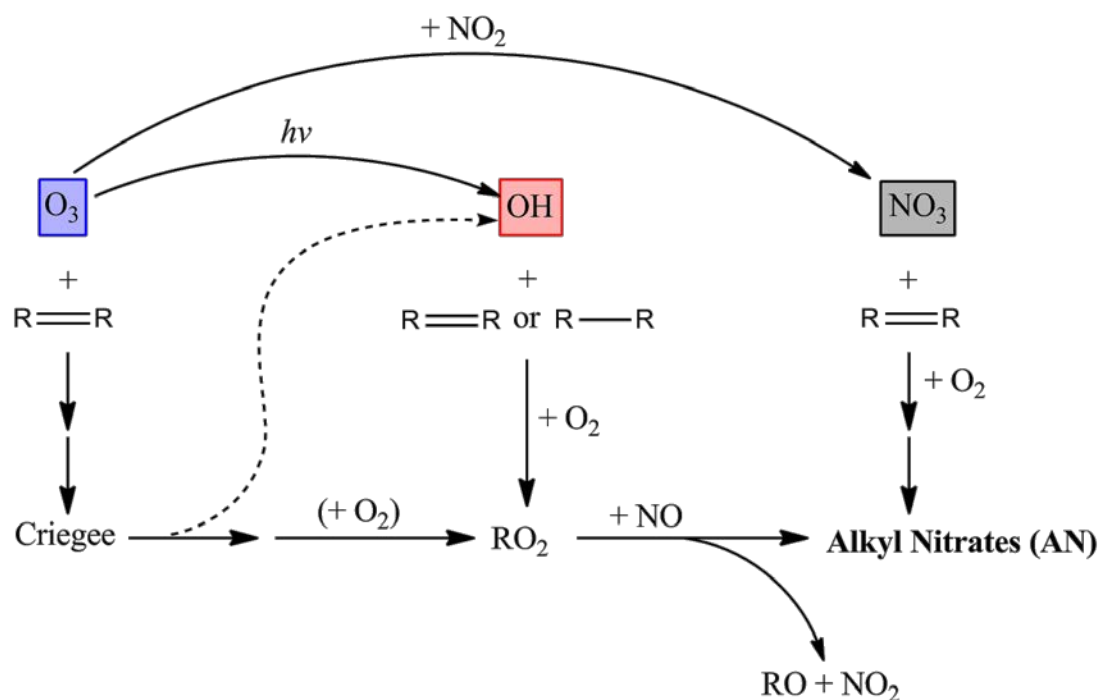


Figure 1. Schematic diagram illustrating the formation of ANs via VOC degradation initiated by NO₃, OH and O₃ reactions.

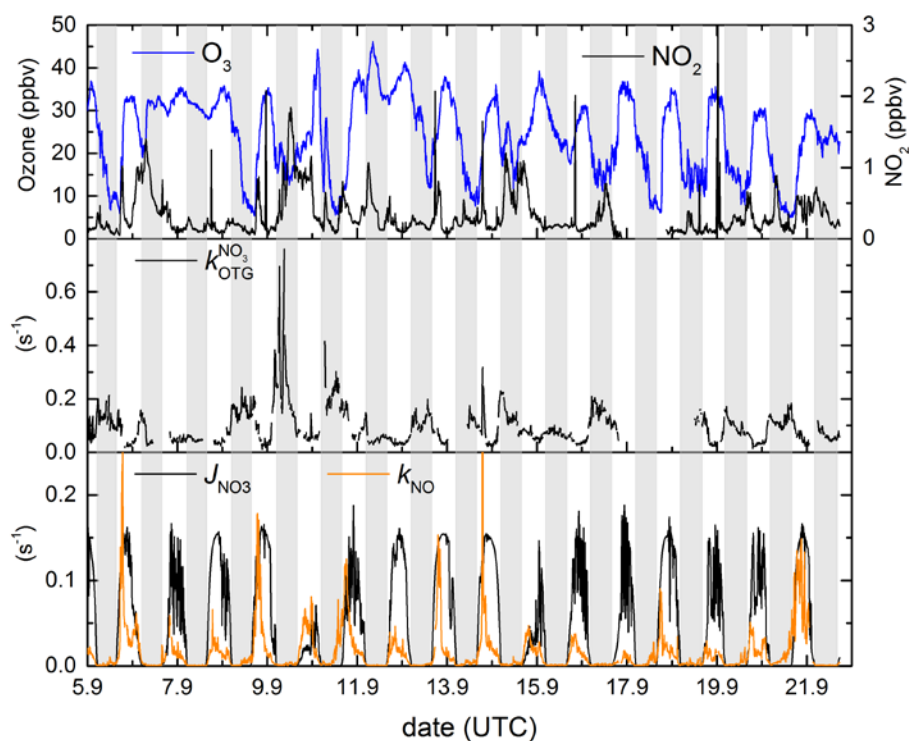


Figure 2. Time series of the NO_3 precursors (NO_2 and O_3), the NO_3 reactivity to organic trace gases ($k_{\text{OTG}}^{\text{NO}_3}$) and the first-order loss-constants for its photolysis (J_{NO_3}) and reaction with NO (k_{NO}) during IBAIRN. Grey shaded regions are night-time.

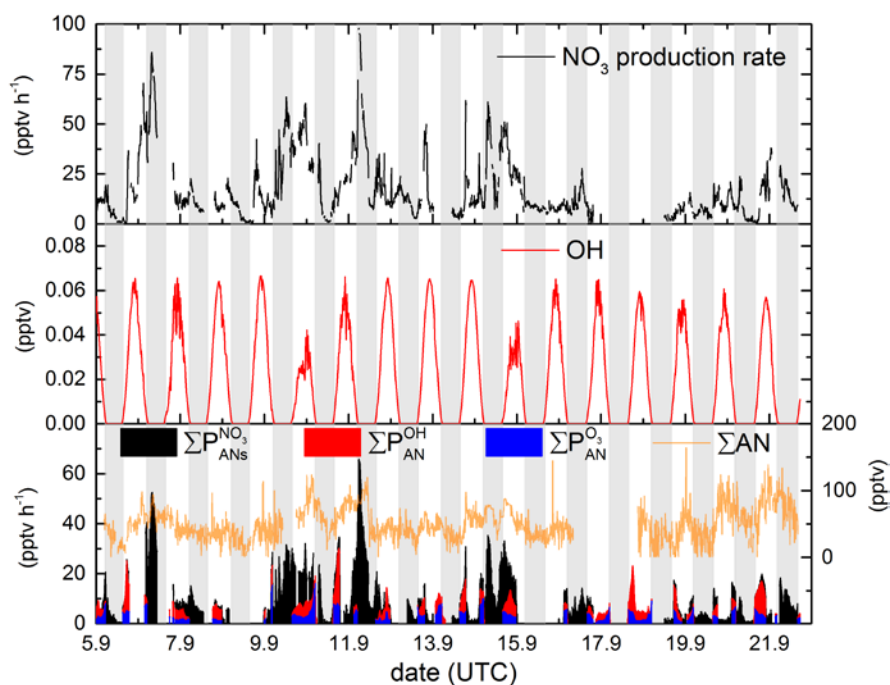


Figure 3. Upper Panel: NO_3 radical production rate from reaction of NO_2 and O_3 . Middle Panel: OH mixing ratio as derived from Eq. 7. Lower Panel: Production rate of ANs from OH (red), O_3 (blue) and NO_3 radicals (black) and the ΣAN mixing ratio (orange line).

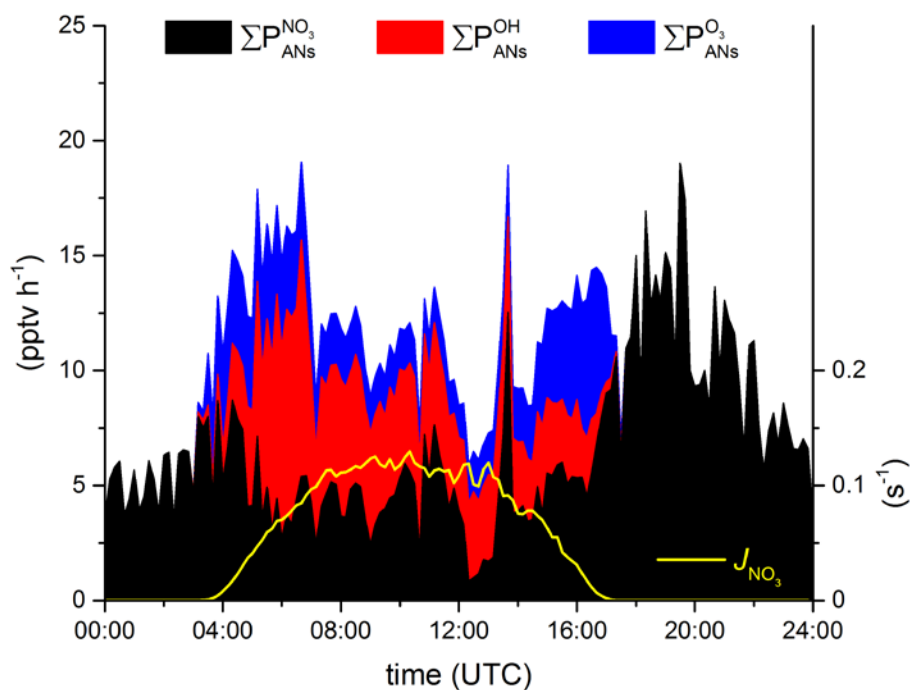


Figure 4. Diel profiles (means) of the AN production rates for VOC initiated oxidation by the OH radical (ΣP_{ANs}^{OH}), O_3 ($\Sigma P_{ANs}^{O_3}$) and the NO_3 radicals ($\Sigma P_{ANs}^{NO_3}$) and the photolysis rate constant of NO_3 (yellow line) to distinguish in between night and day.

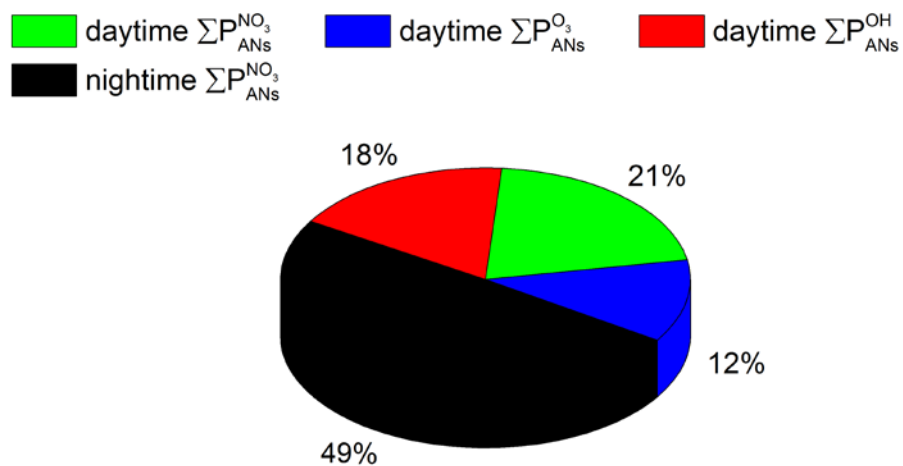


Figure 5. Contribution of NO_3^- , OH^- , and O_3 – initiated degradation of VOCs to the overall formation of alkyl nitrates.

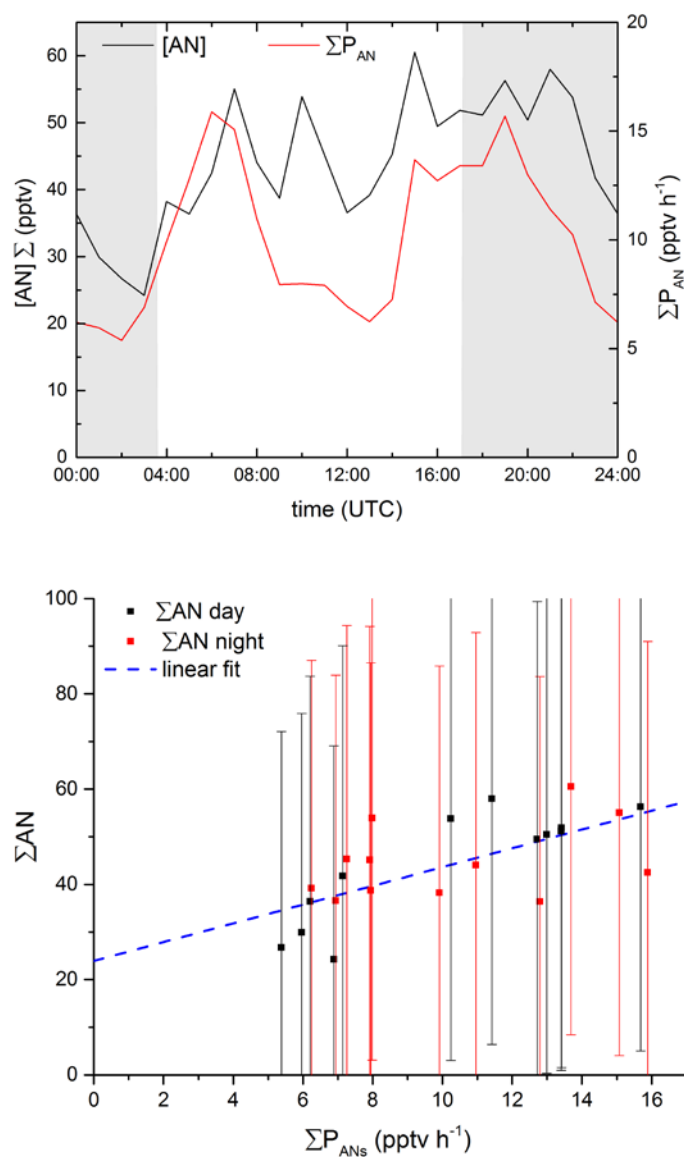


Figure 6: Upper panel: Diel profiles of production rate and mixing ratios of ANs during IBAIRN. Lower panel: Plot of ΣAN mixing ratios versus the total production rate from NO_3^- , OH - and O_3 -initiated VOC oxidation during day (06:00-15:00 UTC, black dots) and night-time (18:00-03:00 UTC, red dots). The slope of the linear fit to the data (blue line) indicates a lifetime of 2 ± 0.5 hr.



5

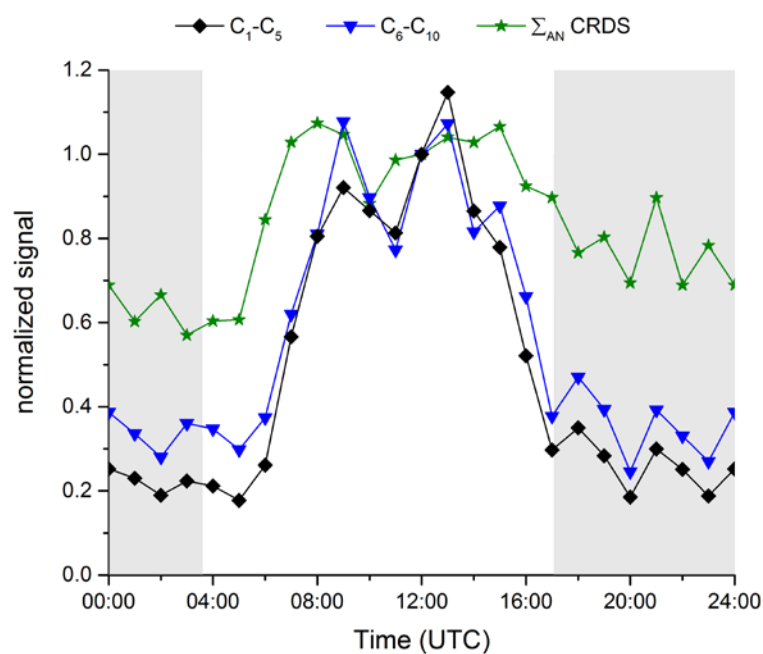


Figure 7. Relative diel profile of I-CIMS signals attributed to C1-C5 and C6-C10 organic nitrates and comparison with ΣANs measured by the TD-CRDS. Data normalized to 1 at 12:00 UTC.

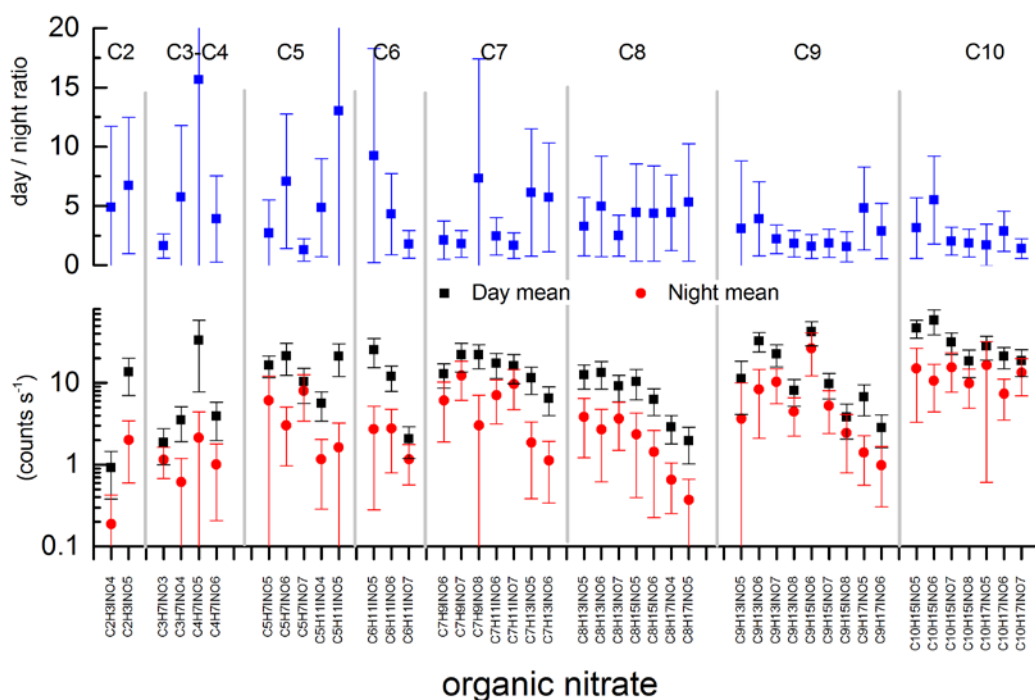


Figure 8. Campaign mean signals for organic nitrates measured by the I-CIMS. The I-CIMS was not calibrated thus only the raw signal (counts per second) at each mass is given.